

## Effect of Adhesive Thickness on the Intensity of Singular Stress at the Adhesive Dissimilar Joint\*

Yu ZHANG\*\*, Nao-Aki NODA\*\*, Ken-Tarou TAKAISI\*\* and Xin LAN\*\*

\*\* Department of Mechanical Engineering, Kyushu Institute of Technology,  
1-1 Sensui-cho, Tobata-ku, Kitakyushu-shi, Fukuoka, Japan  
E-mail:zyzhangyu1225@yahoo.com

### Abstract

This paper deals with the singular stress field at the adhesive dissimilar joint, and discusses the effect of material combination and adhesive thickness on the intensity of the singular stress when bonded strip is subjected to tension. A useful method to calculate the intensity of singular stress at the adhesive dissimilar joint is presented with focusing on the stresses at the edge calculated by finite element method. The intensities of singular stress are indicated in charts with varying adhesive thickness  $t$  under arbitrary material combinations for adhesive and adherents, and it is found that the intensity of singular stress increases with increasing the adhesive thickness  $t$  until  $t=W$ , when  $W$  is the width of adhesive. The intensity of singular stresses are also charted under arbitrary material combinations which are presented by Dunders' parameters  $\alpha$ ,  $\beta$  when  $t/W = 0.001$  and  $t/W = 0.1$ , and it is found that for a fixed value  $\beta$  the intensity of singular stress increases with increasing  $\alpha$  when  $\alpha$  is small while it decreases with increasing  $\alpha$  when  $\alpha$  is large.

**Key words:** Elasticity, Fracture Mechanics, Finite Element Method, Intensity of Singular Stress, Adhesive

### 1. Introduction

Adhesive joints are most frequently used in numerous industrial sectors such as automobile, shipbuilding, aeronautical, etc., replacing or supplementing traditional joining technologies, such as welding or riveting. Moreover, the adhesive joints have also been used for bonding composite restorations to the dental substrate<sup>(1),(2)</sup>. The micro-tensile bond test is a laboratory procedure frequently employed today in an attempt to predict the clinical effectiveness of adhesive used for bonding composite restorations to the dental substrate<sup>(3)</sup>, see Fig.1. This test can be considered as a miniaturized version of the conventional engineering tensile adhesion test using butt-joint specimens, and the specimens can be rectangular in cross-section, see Fig.2.

However, a mismatch of different materials properties may cause stress singularity at the edge of an interface between different materials, which leads to failure of bonding part in structures, and the singularity is expressed by the intensity of singular stress.

So far, many studies have been done to evaluate the strength of adhesive<sup>(4),(5)</sup>, and few studies has been conducted to describe the stress distribution on the interface between the adhesive and adherents used in micro-tensile bond tests<sup>(6)</sup>. Besides, until now, no study has obtained the intensity of singular stress at the edge of adhesive joint in micro-tensile bond tests.

From previous experimental results, it is found that the joint strength decreases with increasing of adhesive thickness<sup>(7)</sup>. However, the reason why the joint strength decreases with increasing of adhesive thickness has not been explained explicitly.

\*Received 22 Apr., 2010 (No. 10-0175)  
[DOI: 10.1299/jmmp.4.1467]

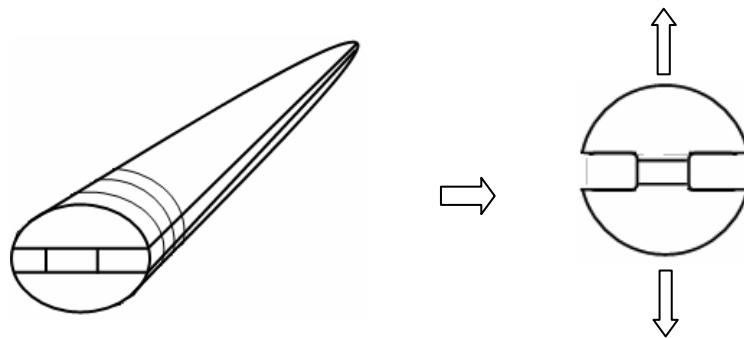


Fig.1 Micro-tensile bond test.

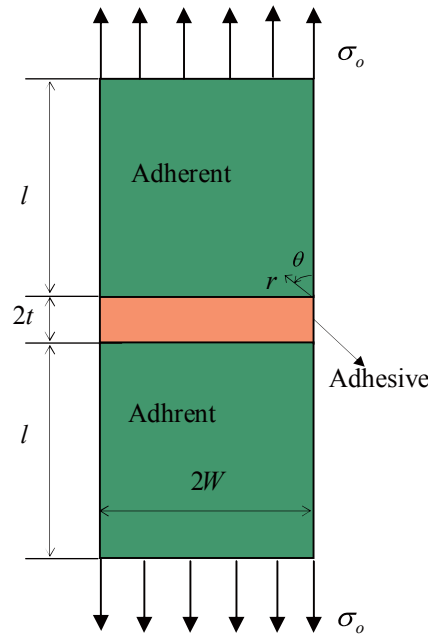


Fig.2 Adhesive joint

Therefore, in this paper, to explain the reason by simulation, the effect of adhesive thickness on the intensity of singular stress will be analyzed by the finite element method, also the effect of material combination on the intensity of singular stress will be analyzed.

## 2. Method of analysis of the intensity of singular stress

For the adhesive joint as shown in Fig.2, it is known that the interface stress  $\sigma_{ij}$  ( $ij = rr, \theta\theta, r\theta$ ) goes to infinity at the edge of joint and has singularity of  $\sigma_{ij} \propto 1/r^{1-\lambda}$  when  $\alpha(\alpha - 2\beta) > 0$ ; here,  $\alpha, \beta$  are Dunders' parameters which are expressed by Poisson's ratio  $\nu$  and shear modulus  $G$ . The singularity index  $\lambda$  at the joint of interface can be expressed by the following equation<sup>(8),(9)</sup>. Table 1 shows the values  $\lambda$  obtained by solving Eq.(1). It can be found that  $\lambda < 1$  when  $\alpha(\alpha - 2\beta) > 0$ ;  $\lambda = 1$  when  $\alpha(\alpha - 2\beta) = 0$ ;  $\lambda > 1$  when  $\alpha(\alpha - 2\beta) < 0$ .

$$\left[ \sin^2\left(\frac{\pi}{2}\lambda\right) - \lambda^2 \right]^2 \beta^2 + 2\lambda^2 \left[ \sin^2\left(\frac{\pi}{2}\lambda\right) - \lambda^2 \right] \alpha\beta + \lambda^2(\lambda^2 - 1)\alpha^2 + \frac{\sin^2(\lambda\pi)}{4} = 0 \quad (1)$$

$$\alpha = \frac{G_1(\kappa_2 + 1) - G_2(\kappa_1 + 1)}{G_1(\kappa_2 + 1) + G_2(\kappa_1 + 1)} \quad \beta = \frac{G_1(\kappa_2 - 1) - G_2(\kappa_1 - 1)}{G_1(\kappa_2 + 1) + G_2(\kappa_1 + 1)} \quad (2)$$

$$\kappa_j = \begin{cases} \frac{3-\nu_j}{1+\nu_j} (\text{plane stress}) \\ 3-4\nu_j (\text{plane strain}) \end{cases}, \kappa_j = (j=1,2) \quad (3)$$

The intensity of singular stress  $K_\sigma$  at the adhesive dissimilar joint is expressed as  $K_\sigma = \lim_{r \rightarrow 0} [r^{1-\lambda} \times \sigma_{\theta|\theta=\pi/2}(r)]$  (4) and the dimensionless of intensity of singular stress  $F_\sigma$  is defined by the following equation.

$$F_\sigma = \frac{K_\sigma}{\sigma(2W)^{1-\lambda}} = \frac{\lim_{r \rightarrow 0} [r^{1-\lambda} \sigma_{\theta|\theta=\pi/2}(r)]}{\sigma(2W)^{1-\lambda}} \quad (5)$$

Here,  $\sigma$  is the stress applying to the  $y$  direction.

Table 1 Values of singular index  $\lambda$

[ Red figures indicate  $\lambda < 1$ , blue figures indicate  $\lambda > 1$ , black figures indicate  $\lambda = 1$  ]

$\alpha$	$\beta=-0.45$	$\beta=-0.4$	$\beta=-0.3$	$\beta=-0.2$	$\beta=-0.1$	$\beta=0$	$\beta=0.1$	$\beta=0.2$	$\beta=0.3$	$\beta=0.4$	$\beta=0.45$
-1.00	0.87624	0.8073	0.7205	0.6646	0.6247	0.5946					
-0.95	0.9349	0.8536	0.7576	0.6975	0.6550	0.6232					
-0.90	1.00000	0.9008	0.7941	0.7295	0.6845	0.6511					
-0.80		1.0000	0.8655	0.7916	0.7415	0.7048					
-0.70		1.1174	0.9348	0.8510	0.7961	0.7564					
-0.60			1.0000	0.9071	0.8480	0.8060	0.7746				
-0.50			1.0558	0.9580	0.8966	0.8532	0.8210				
-0.40			1.0913	1.0000	0.9403	0.8974	0.8655				
-0.30			1.0964	1.0276	0.9761	0.9371	0.9075				
-0.20			1.0756	1.0360	1.0000	0.9699	0.9457	0.9269			
-0.10				1.0251	1.0083	0.9921	0.9777	0.9659			
0.00				1.0000	1.0000	1.0000	1.0000	1.0000			
0.10				0.9659	0.9777	0.9921	1.0083	1.0251			
0.20				0.9269	0.9457	0.9699	1.0000	1.0360	1.0756		
0.30					0.9075	0.9371	0.9761	1.0276	1.0964		
0.40					0.8655	0.8974	0.9403	1.0000	1.0913		
0.50					0.8210	0.8532	0.8966	0.9580	1.0558		
0.60					0.7746	0.8060	0.8480	0.9071	1.0000		
0.70						0.7564	0.7961	0.8510	0.9348	1.1174	
0.80						0.7048	0.7415	0.7916	0.8655	1.0000	
0.90						0.6511	0.6845	0.7295	0.7941	0.9008	1.0000
0.95						0.6232	0.6550	0.6975	0.7576	0.8536	0.9349
1.00						0.5946	0.6247	0.6646	0.7205	0.8073	0.8762

In this paper, the finite element method is used to obtain the stress at the joint of interface, and the software is MSC.MARC 2007. Because of symmetry, one-fourth portion of Fig.2 is analyzed as a model for analysis. Here,  $E_1, \nu_1$  are the Young's modulus and the Poisson's ratio of the adherent, and  $E_2, \nu_2$  are the Young's modulus and the Poisson's ratio of the adhesive. The width of the model  $2W=2000\text{mm}$ , and the length  $l = 2W$  because it is demonstrated that when  $l \geq 2W$  the interface stresses are the same. The adhesive thickness is changed as  $t/W = 0.001, 0.01, 0.1, 0.5, 1, 2, 4$ .

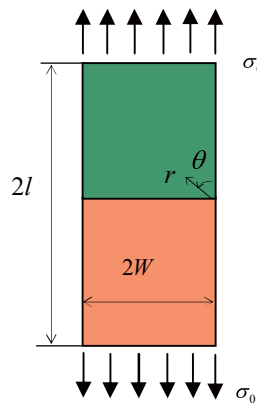


Fig.3 Bonded strip

We will propose the method of calculating the intensity of singular stress from the results of FEM. In this paper, the ratio of intensity of singular stress  $K_\sigma^1/K_\sigma^2$  will be considered. Here, the superscripts 1, 2 mean specific problems whose  $t/W$  are distinct. As shown in Eqs. (4), (5), the dimensionless intensity of singular stress is related to the distance  $r$ , singular index  $\lambda$ , and stress  $\sigma_0$ , width  $W$  and limiting stress  $\lim_{r \rightarrow 0} \sigma_{\theta|\theta=\pi/2}$ . Consider different adhesive thicknesses  $t_1, t_2$  as problem 1 and problem 2, both of which have the same stress at infinity  $\sigma$  and material combinations. Therefore, it should be noted that the singular index  $\lambda_1 = \lambda_2$ . As shown in Eq. (6), the ratio of intensity of singular stress  $K_\sigma^1/K_\sigma^2$  is controlled by the ratio of stress  $\lim_{r \rightarrow 0} (\sigma_{\theta|\theta=\pi/2}^1 / \sigma_{\theta|\theta=\pi/2}^2)$ .

$$\frac{K_\sigma^1}{K_\sigma^2} = \frac{\sigma^1 (2W)^{1-\lambda_1} F_\sigma^1}{\sigma^2 (2W)^{1-\lambda_2} F_\sigma^2} = \frac{F_\sigma^1}{F_\sigma^2} = \lim_{r \rightarrow 0} \frac{\left[ r^{1-\lambda_1} \sigma_{\theta|\theta=\pi/2}^1(r) \right]}{\left[ r^{1-\lambda_2} \sigma_{\theta|\theta=\pi/2}^2(r) \right]} = \lim_{r \rightarrow 0} \frac{\sigma_{\theta|\theta=\pi/2}^1(r)}{\sigma_{\theta|\theta=\pi/2}^2(r)} \quad (6)$$

Therefore, in this paper, the ratio of intensity of singular stress is mainly considered in the analysis. To obtain the intensity of singular stress from the ratio, a reference problem as shown in Fig.3 will be used because the intensity of singular stress has been investigated.

### 3. Interface Stress distribution and ratio of the distributions obtained by using FEM

Figure 4 shows the stress distribution on the interface between adhesive and adherent when adhesive thickness  $t/W = 1$  and  $\alpha = 0.8, \beta = 0.1, \alpha = 0.9, \beta = 0.3, \alpha = 0.3, \beta = 0, \alpha = 0.2, \beta = 0.1, \alpha = 0.2, \beta = 0.2$ . It is confirmed that when  $\alpha(\alpha - 2\beta) > 0$ , the stress at the edge goes to infinite with different intensity depending on  $\alpha, \beta$ ; stress goes to constant when  $\alpha(\alpha - 2\beta) = 0$ ; stress goes to 0 when  $\alpha(\alpha - 2\beta) < 0$ . In this analysis, those stress distributions along the interface are obtained by extrapolation from the results for adherent and adhesive. Usually, those FEM results do not coincide with each other; and therefore, the average values are used to plot the stress distribution.

To understand the effect of adhesive thickness on the intensity of singular stress, the stress distributions with different adhesive thickness are considered. Figure 5 (a) shows the stress distribution on the interface when  $\alpha = 0.3, \beta = 0$  with adhesive thickness  $t/W$  changed from 0.001, to 0.01, 0.1, 0.5, 1, 2, 4, and to see the detail of singular stress distribution at the edge of the interface, the magnified figure is shown in Fig.5 (b). It is found that the increase of adhesive thickness causes a significant increase of stress singularity area. When  $t/W = 1, 2, 4$ , the stress distribution is almost the same. More detail stress distributions at the edge of interface under different adhesive thickness is shown in Fig.5 (c). It is seen that the stresses become large suddenly. Real stresses should go to infinity at  $r \rightarrow 0$ , although FEM cannot express the singular stresses. More important discovery is that all the lines are parallel to each other along  $r/W$ .

Figure 6 shows the ratio  $\sigma_y^1 / \sigma_y^1|_{t/W=1}$  near the edge of adhesive joint when the smallest mesh size is  $1/3^8 = 1/6561 \text{ mm}$  with  $W = 1000 \text{ mm}$ , and it should be noted that all lines are constant. Although the singularity at the edge is difficult to be described by FEM, the ratio  $\sigma_y^1 / \sigma_y^1|_{t/W=1}$  shown in Fig.6 can be accurate even in the singularity regions.

To see the discovery more deeply, Table2(a) compares the stress distributions and the ratio of the results obtained by using FEM with the smallest mesh size  $1/3^8 = 1/6561 \text{ mm}$ . It is found that the ratio is almost constant by 4 digit independent of  $r$ . Table 2(b) shows the results with the smallest mesh size  $1/3^4 = 1/81 \text{ mm}$ . In this case, it is found that the values are almost constant by 3 digit independent of  $r$ . It is also found that the ratio in Table 2(a) and (b) coincide each other by 3 digit. Although real interface singular stresses cannot be expressed easily by using the FEM because the values of stress largely depend on the mesh size, it is found that the ratio of stress can be obtained vary accurately as shown in Table 2. In other words, the ratio of interface stress is nearly independent of mesh size.

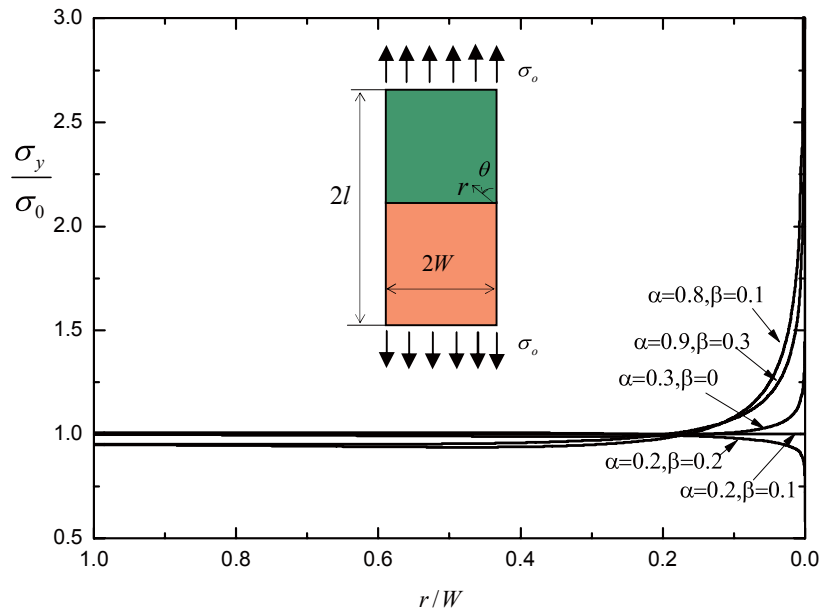
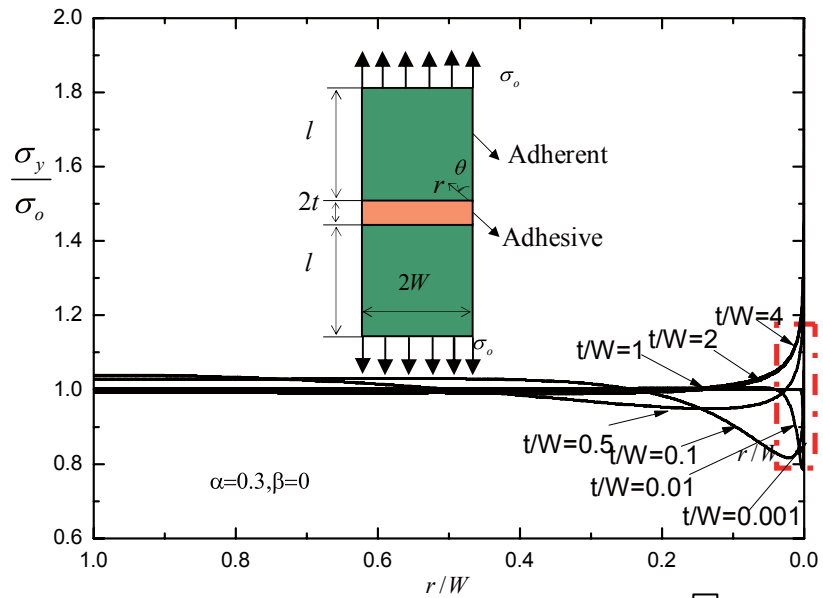
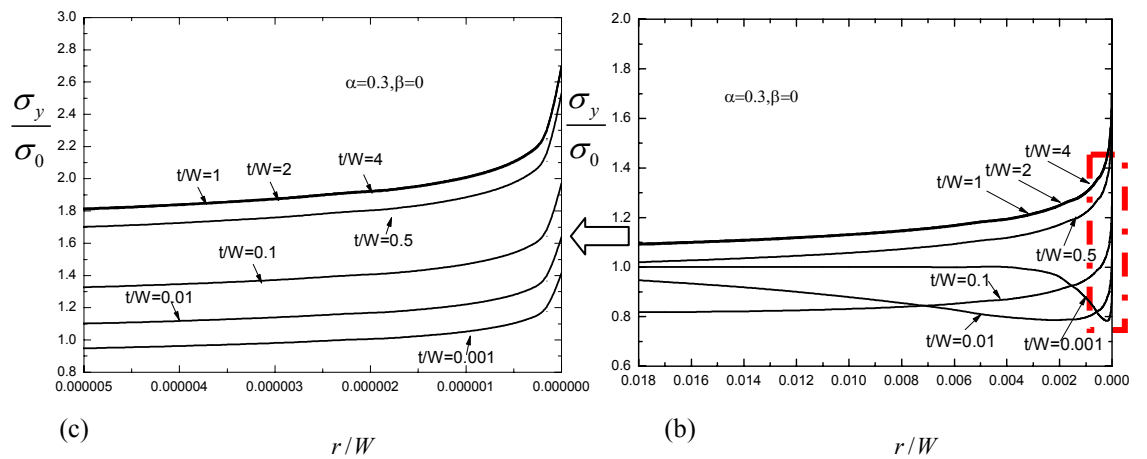


Fig.4 The stress distribution on the interface with different material combination.



(a)



(c)

(b)

Fig.5 Stress distribution  $\sigma_y$  on the interface with different adhesive thickness.



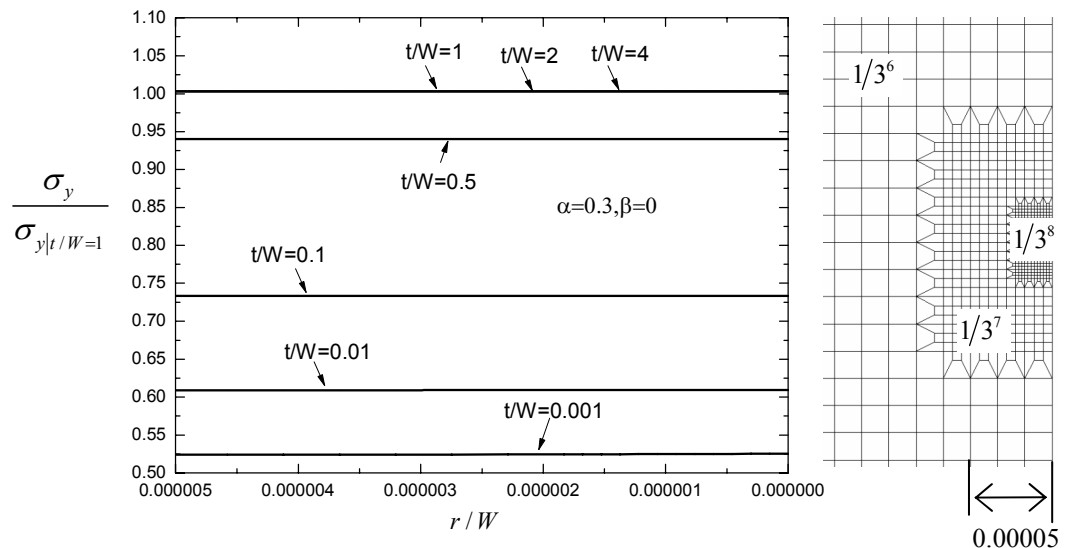


Fig. 6 Ratio of  $\sigma_y / \sigma_{y|t/W=1}$  near the edge of adhesive joint.

Table 2 Stress distribution  $\sigma_y$  along the interface when  $\alpha = 0.3, \beta = 0$ . The ratio of stress distributions  $\sigma_y / \sigma_{y|t/W=1}$  are indicated in parentheses.

(a)  $\sigma_y$  and  $(\sigma_y / \sigma_{y|t/W=1})$  obtained with the smallest mesh size  $1/3^8 = 1/6561mm$  and  $W = 1000mm$

$r/W \backslash t/W$	0.001	0.01	0.1	0.5	1	2	4
$\rightarrow 0$	1.414(0.525)	1.640(0.609)	1.973(0.733)	2.530(0.940)	2.692(1.000)	2.700(1.003)	2.670(1.003)
1/6561000	1.177(0.525)	1.365(0.609)	1.644(0.733)	2.108(0.940)	2.242(1.000)	2.249(1.003)	2.249(1.003)
2/6561000	1.138(0.525)	1.320(0.609)	1.589(0.733)	2.038(0.940)	2.167(1.000)	2.174(1.003)	2.174(1.003)
3/6561000	1.109(0.525)	1.286(0.609)	1.548(0.733)	1.985(0.940)	2.111(1.000)	2.118(1.003)	2.117(1.003)
4/6561000	1.088(0.525)	1.262(0.609)	1.519(0.733)	1.948(0.940)	2.072(1.000)	2.078(1.003)	2.078(1.003)
5/6561000	1.071(0.525)	1.243(0.609)	1.497(0.733)	1.919(0.940)	2.041(1.000)	2.047(1.003)	2.047(1.003)
6/6561000	1.058(0.525)	1.228(0.609)	1.478(0.733)	1.896(0.940)	2.016(1.000)	2.022(1.003)	2.022(1.003)
7/6561000	1.047(0.525)	1.215(0.609)	1.463(0.733)	1.876(0.940)	1.995(1.000)	2.002(1.003)	2.001(1.003)
8/6561000	1.038(0.525)	1.205(0.609)	1.450(0.733)	1.859(0.940)	1.978(1.000)	1.984(1.003)	1.984(1.003)
9/6561000	1.030(0.525)	1.195(0.609)	1.439(0.733)	1.845(0.940)	1.962(1.000)	1.968(1.003)	1.968(1.003)

(b)  $\sigma_y$  and  $(\sigma_y / \sigma_{y|t/W=1})$  obtained with the smallest mesh size  $1/3^4 = 1/81mm$  and  $W = 1000mm$

$r/W \backslash t/W$	0.001	0.01	0.1	0.5	1	2	4
$\rightarrow 0$	1.072(0.524)	1.246(0.609)	1.499(0.733)	1.923(0.940)	2.045(1.000)	2.051(1.003)	2.051(1.003)
1/81000	0.889(0.522)	1.036(0.609)	1.249(0.733)	1.601(0.940)	1.703(1.000)	1.708(1.003)	1.708(1.003)
2/81000	0.859(0.522)	1.001(0.608)	1.207(0.733)	1.548(0.940)	1.647(1.000)	1.652(1.003)	1.652(1.003)
3/81000	0.838(0.522)	0.975(0.608)	1.176(0.733)	1.508(0.940)	1.604(1.000)	1.609(1.003)	1.608(1.003)
4/81000	0.824(0.523)	0.956(0.608)	1.154(0.733)	1.480(0.940)	1.574(1.000)	1.579(1.003)	1.579(1.003)
5/81000	0.813(0.525)	0.942(0.607)	1.137(0.733)	1.458(0.940)	1.551(1.000)	1.555(1.003)	1.555(1.003)
6/81000	0.806(0.526)	0.930(0.607)	1.123(0.733)	1.440(0.940)	1.532(1.000)	1.536(1.003)	1.536(1.003)
7/81000	0.800(0.528)	0.920(0.607)	1.111(0.733)	1.425(0.940)	1.516(1.000)	1.521(1.003)	1.520(1.003)
8/81000	0.795(0.529)	0.912(0.607)	1.092(0.733)	1.403(0.940)	1.502(1.000)	1.507(1.003)	1.507(1.003)
9/81000	0.792(0.531)	0.904(0.607)	1.084(0.733)	1.401(0.940)	1.491(1.000)	1.495(1.003)	1.495(1.003)

As explained in the chapter 2, the ratio  $K_\sigma^1/K_\sigma^2$  is equal to the ratio  $\sigma_y^1/\sigma_y^2$  along  $r$ , and as shown in Table 2 since the ratio  $\sigma_y^1/\sigma_y^2$  along  $r$  is independent of  $r$ , only the stress  $\sigma_y$  of the first element should be considered.

In the following of the paper, the stress intensity factors for known reference problem 2  $K_\sigma^2$  will be shown and the stress intensity factors for unknown problem 1  $K_\sigma^1$  will be discussed from the ratio  $K_\sigma^1/K_\sigma^2$ .

#### 4. Intensity of singular stress for bonded strip as a reference solution

In the previous chapters, it is found that the ratio of interface stress distribution can be given very accurately by using FEM. However, to obtain the intensity of singular stress, a reference solution is necessary. Chen-Nisitani<sup>(10)</sup> and Noda et. al<sup>(11)</sup> have analyzed the intensity of singular stress in a bonded strip in Fig.3 accurately by using the body force method. Table 3 and Fig.7 indicate the results for bonded strip, which are equivalent to the case  $t/W \geq 1$ . In the previous studies<sup>(10),(11)</sup>, only the results for singular stress  $\lambda > 1$  are indicated, and the results<sup>(11)</sup> are used in Table 3 and Fig.7. However, in this study, all material combinations are newly considered; and, therefore Fig.7 includes new results for  $F_\sigma > 1$  where no singular stress because singular index  $\lambda > 1$ . Those new results are obtained easily by FEM because of no singularity stress. However, the dashed lines are extended from solid lines because some special material combination are difficult to be obtained by using commercial FEM codes. In this paper, intensity of singular stress will be shown as the ratio  $F_\sigma / F_{\sigma|t/W=1}$ .

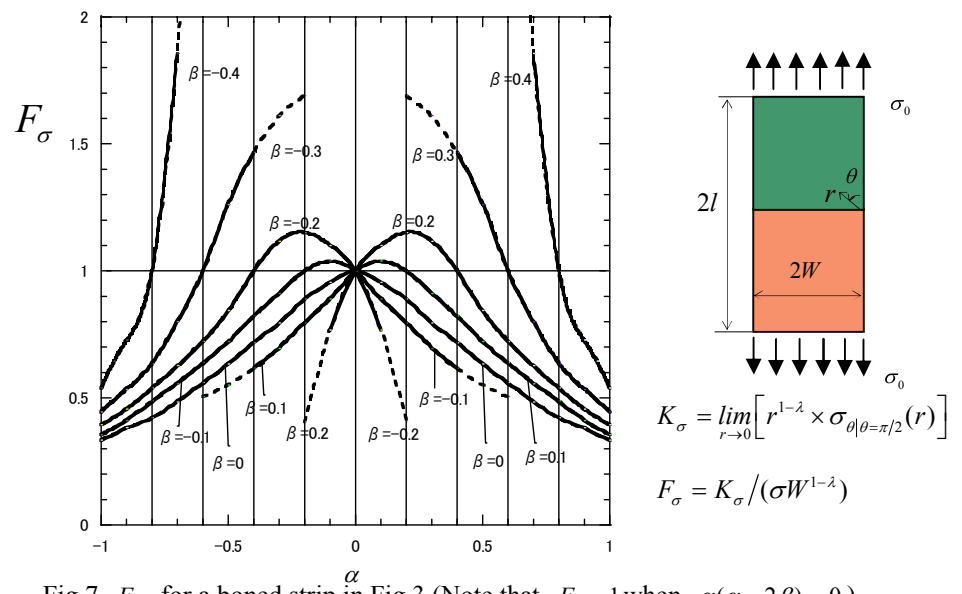


Fig.7  $F_\sigma$  for a boned strip in Fig.3 (Note that  $F_\sigma = 1$  when  $\alpha(\alpha - 2\beta) = 0$ )

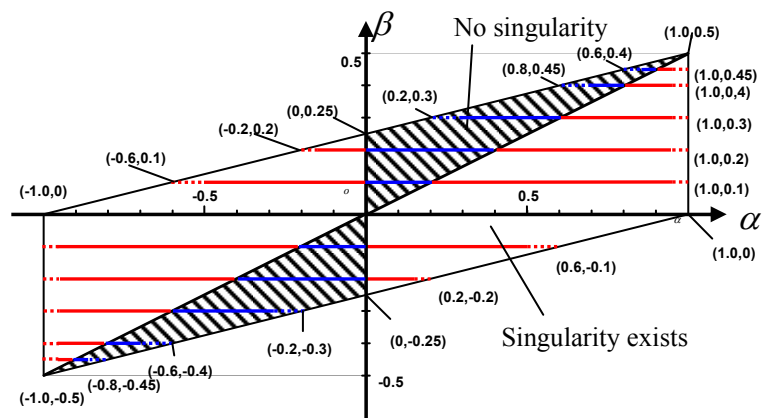


Fig.8 The map of  $\alpha$  and  $\beta$

Table 3  $F_\sigma$  at interface edge point in bonded finite plate  
[ ( ): Extrapolated or interpolated results. Red figures indicate  $\lambda < 1$ , blue figures indicate  $\lambda > 1$ , black figures indicate  $\lambda = 1$  ]

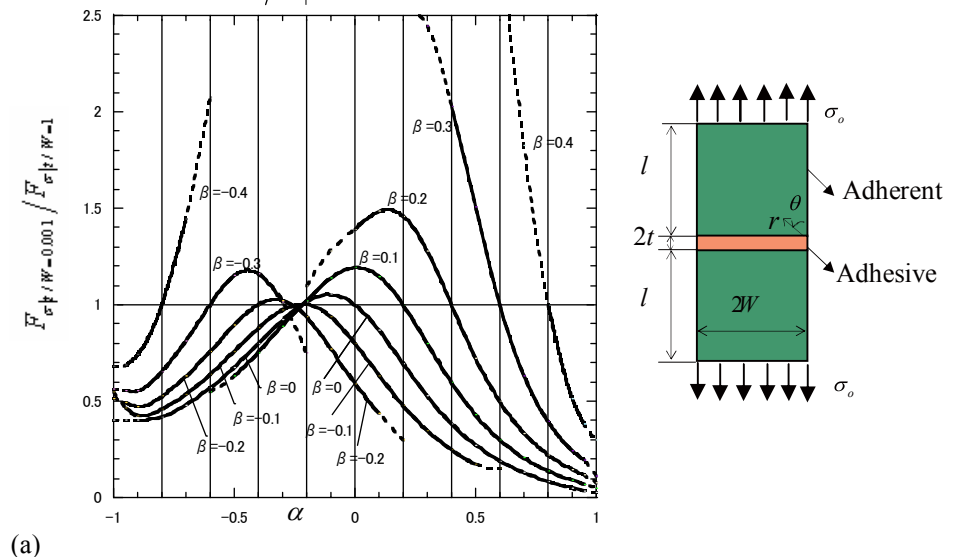
$\alpha$	$\beta=-0.4$	$\beta=-0.3$	$\beta=-0.2$	$\beta=-0.1$	$\beta=0$	$\beta=0.1$	$\beta=0.2$	$\beta=0.3$	$\beta=0.4$
1.00	0.540	0.446	0.395	0.357	0.332	--	--	--	--
-0.95	0.643	(0.349)	(0.381)	(0.422)	(0.491)	--	--	--	--
-0.90	0.726	0.534	0.456	0.412	0.381	--	--	--	--
-0.80	1.000	0.636	0.538	0.487	0.45	--	--	--	--
-0.70	(1.855)	0.800	0.626	0.558	0.486	--	--	--	--
-0.60	(3.291)	1.000	0.724	0.638	0.559	(0.505)	--	--	--
-0.50	--	1.264	0.842	0.722	0.635	(0.551)	--	--	--
-0.40	--	1.467	1.000	0.822	0.718	0.615	--	--	--
-0.30	--	(1.609)	1.118	0.913	0.796	0.697	--	--	--
-0.20	--	(1.690)	1.153	1.000	0.889	0.797	(0.404)	--	--
-0.10	--	--	1.103	1.037	0.955	0.890	0.767	--	--
0.00	--	--	1.000	1.000	1.000	1.000	1.000	--	--
0.10	--	--	0.767	0.890	0.955	1.037	1.103	--	--
0.20	--	--	(0.404)	0.797	0.889	1.000	1.153	(1.690)	--
0.30	--	--	--	0.697	0.796	0.913	1.118	(1.609)	--
0.40	--	--	--	0.615	0.718	0.822	1.000	1.467	--
0.50	--	--	--	(0.551)	0.635	0.722	0.842	1.264	--
0.60	--	--	--	(0.505)	0.559	0.638	0.724	1.000	(3.291)
0.70	--	--	--	--	0.486	0.558	0.626	0.800	1.855
0.80	--	--	--	--	0.450	0.487	0.538	0.636	1.000
0.90	--	--	--	--	0.381	0.412	0.456	0.534	0.726
0.95	--	--	--	--	(0.491)	(0.422)	(0.381)	(0.349)	0.643
1.00	--	--	--	--	0.332	0.357	0.395	0.446	0.540

**5. Results and Discussion**

**5.1 Effect of material combination on generalized stress intensity factors**

As discussed before, it is found that the ratio  $F_\sigma^1/F_\sigma^2$  is equivalent to the ratio  $\sigma_y^1/\sigma_y^2$  along interface  $r$ . By calculating the ratio  $\sigma_y/\sigma_{y|t/W=1}$  around the edge of interface, the ratio  $F_\sigma/F_{\sigma|t/W=1}$  has been obtained for all material combinations. Figure 8 shows the map of  $\alpha$  and  $\beta$  used for this calculations.

Figure 9 shows  $F_\sigma/F_{\sigma|t/W=1}$  with varying  $\alpha$  and  $\beta$  when (a)  $t/W = 0.001$ ; (b)  $t/W = 0.1$ , and Table 4 gives the value for Fig.9. It can be seen that  $F_\sigma/F_{\sigma|t/W=1}$  increases with increasing of  $\alpha$  when  $\alpha$  is small. On the other hand, the ratio  $F_\sigma/F_{\sigma|t/W=1}$  decreases with increasing of  $\alpha$  when  $\alpha$  is large. Comparing the results of  $t/W = 0.001$  and  $t/W = 0.1$ , it is found that the range of the ratio is different; that is, for  $t/W = 0.001$ , the ratio  $F_\sigma/F_{\sigma|t/W=1}$  is widely distributed in the range of 0.025 ~ 2.857, while for  $t/W = 0.1$ , the ratio  $F_\sigma/F_{\sigma|t/W=1}$  is in the small range of 0.185 ~ 1.498.





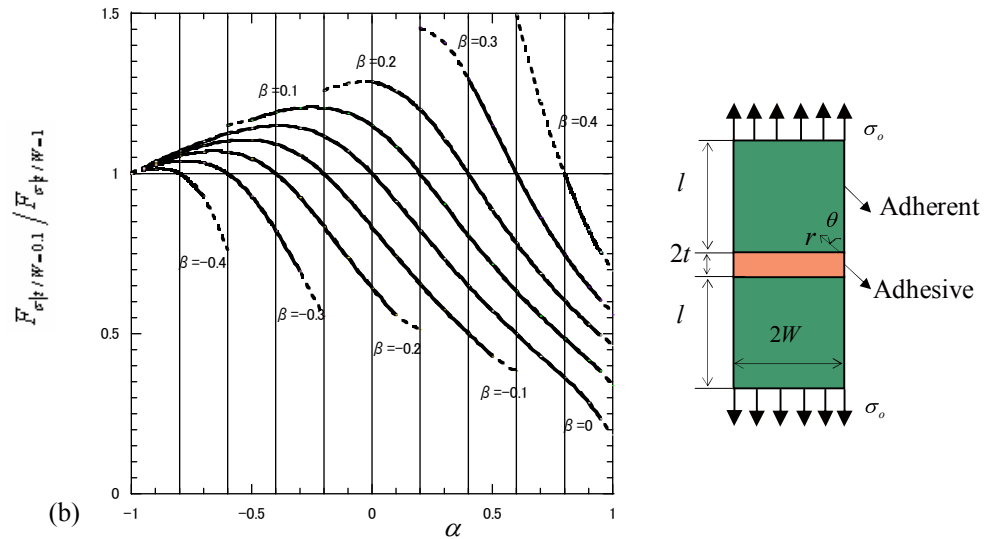


Fig.9  $F_{\sigma} / F_{\sigma|t/W=1}$  with varying  $\alpha$  and  $\beta$  when (a)  $t/W = 0.001$ ; (b)  $t/W = 0.1$

Table 4  $F_{\sigma} / F_{\sigma|t/W=1}$  with varying  $\alpha$  and  $\beta$  when (a)  $t/W = 0.001$ ; (b)  $t/W = 0.1$

(a)  $t/W = 0.001$  (Note that  $F_{\sigma} / F_{\sigma|t/W=1} = 1$  when  $\alpha = 2\beta$ )

[ ( ): Extrapolated or interpolated results. Red figures indicate  $\lambda < 1$ , blue figures indicate  $\lambda > 1$ , black figures indicate  $\lambda = 1$  ]

$\alpha$	$\beta = -0.4$	$\beta = -0.3$	$\beta = -0.2$	$\beta = -0.1$	$\beta = 0$	$\beta = 0.1$	$\beta = 0.2$	$\beta = 0.3$	$\beta = 0.4$
-1.0	(0.682)	(0.566)	(0.517)	(0.552)	(0.400)	--	--	--	--
-0.95	0.6864	0.5554	0.4957	0.4629	(0.400)	--	--	--	--
-0.9	0.7420	0.5533	0.4722	0.4252	0.4004	--	--	--	--
-0.8	1.0000	0.6535	0.5254	0.4587	0.4190	--	--	--	--
-0.7	1.4465	0.8130	0.6289	0.5356	0.4812	--	--	--	--
-0.6	(2.073)	1.0000	0.7579	0.6390	0.5690	(0.550)	--	--	--
-0.5	--	1.1509	0.8952	0.7587	0.6769	0.6297	--	--	--
-0.4	--	1.1613	1.0000	0.8794	0.7988	0.7530	--	--	--
-0.3	--	1.0165	1.0232	0.9725	0.9205	0.8924	--	--	--
-0.2	--	(0.750)	0.9346	1.0000	1.0169	1.0203	(1.100)	--	--
-0.1	--	--	0.7716	0.9372	1.0526	1.1374	(1.280)	--	--
0	--	--	0.5912	0.7994	1.0000	1.1925	1.3925	--	--
0.1	--	--	0.4363	0.6331	0.8665	1.1473	1.4837	--	--
0.2	--	--	(0.300)	0.4768	0.6938	1.0000	1.4608	(2.524)	--
0.3	--	--	--	0.3477	0.5253	0.7974	1.2786	(2.443)	--
0.4	--	--	--	0.2478	0.3834	0.5962	1.0000	2.0311	--
0.5	--	--	--	0.1728	0.2729	0.4281	0.7223	1.5100	--
0.6	--	--	--	(0.150)	0.1904	0.2996	0.4984	1.0000	(2.857)
0.7	--	--	--	--	0.1297	0.2058	0.3355	0.6323	(1.825)
0.8	--	--	--	--	0.0852	0.1388	0.2224	0.3942	1.0000
0.9	--	--	--	--	0.0511	0.0913	0.1456	0.2448	0.5173
0.95	--	--	--	--	0.0348	0.0725	0.1172	0.1930	0.3806
1.0	--	--	--	--	(0.025)	(0.050)	(0.080)	(0.110)	(0.300)

Using the results  $F_{\sigma} / F_{\sigma|t/W=1}$  in Table 4 and  $F_{\sigma|t/W=1}$  in Table 3,  $F_{\sigma}$  are obtained and shown in Fig.10 for  $t/W = 0.001$  and  $t/W = 0.1$

(b)  $t/W = 0.1$  (Note that  $F_\sigma/F_{\sigma|t/W=1} = 1$  when  $\alpha = 2\beta$ )

[ ( ): Extrapolated or interpolated results. Red figures indicate  $\lambda < 1$ , blue figures indicate  $\lambda > 1$ , black figures indicate  $\lambda = 1$  ]

$\alpha$	$\beta=-0.4$	$\beta=-0.3$	$\beta=-0.2$	$\beta=-0.1$	$\beta=0$	$\beta=0.1$	$\beta=0.2$	$\beta=0.3$	$\beta=0.4$
-1	(1.000)	(1.000)	(1.000)	(1.000)	(1.000)	--	--	--	--
-0.95	1.0099	1.0143	1.0164	1.0177	(1.018)	--	--	--	--
-0.9	1.0144	1.0260	1.0312	1.0342	1.0365	--	--	--	--
-0.8	1.0000	1.0390	1.0548	1.0637	1.0698	--	--	--	--
-0.7	0.9275	1.0333	1.0681	1.0870	1.0993	--	--	--	--
-0.6	(0.764)	1.0000	1.0671	1.1018	1.1239	(1.150)	--	--	--
-0.5	--	0.9298	1.0462	1.1048	1.1415	1.1686	--	--	--
-0.4	--	0.8228	1.0000	1.0916	1.1491	1.1910	--	--	--
-0.3	--	0.6943	0.9269	1.0575	1.1426	1.2051	--	--	--
-0.2	--	(0.552)	0.8345	1.0000	1.1175	1.2051	(1.260)	--	--
-0.1	--	--	0.7361	0.9219	1.0698	1.1890	(1.280)	--	--
0	--	--	0.6433	0.8324	1.0000	1.1501	1.2864	--	--
0.1	--	--	0.5579	0.7413	0.9144	1.0856	1.2580	--	--
0.2	--	--	(0.513)	0.6548	0.8229	1.0000	1.1994	(1.453)	--
0.3	--	--	--	0.5748	0.7332	0.9037	1.1092	(1.409)	--
0.4	--	--	--	0.5007	0.6492	0.8071	1.0000	1.2962	--
0.5	--	--	--	0.4307	0.5715	0.7160	0.8879	1.1518	--
0.6	--	--	--	(0.382)	0.4994	0.6324	0.7828	1.0000	(1.498)
0.7	--	--	--	--	0.4309	0.5561	0.6882	0.8635	(1.224)
0.8	--	--	--	--	0.3625	0.4855	0.6040	0.7467	1.0000
0.9	--	--	--	--	0.2851	0.4180	0.5291	0.6479	0.8241
0.95	--	--	--	--	0.2329	0.3836	0.4947	0.6046	0.7544
	--	--	--	--	(0.185)	(0.339)	(0.463)	(0.560)	(0.697)

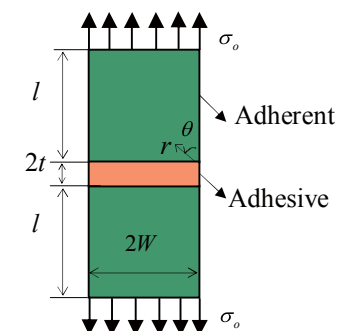
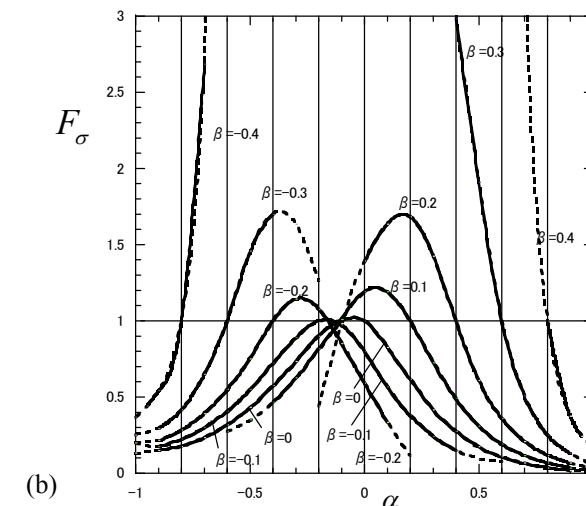
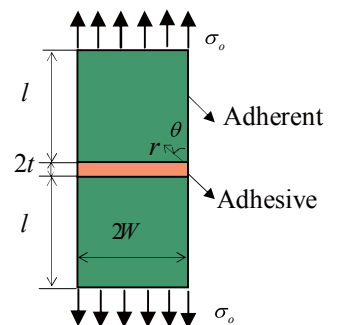
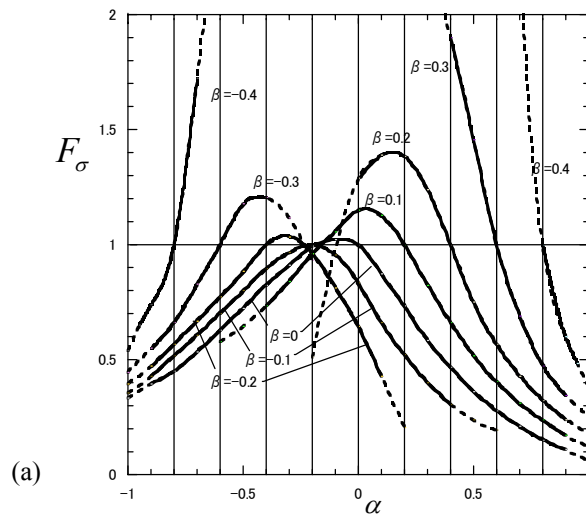


Fig.10  $F_\sigma$  with varying material combination  $\beta$  when (a)  $t/W = 0.001$ ; (b)  $t/W = 0.1$

**5.2 Effect of adhesive thickness on the intensity of singular stress**

To investigate the effect of adhesive thickness on the intensity of singular stresses, stainless steel SUS304, aluminum alloys A7075, silicon and IC substrate FR-4.5 are considered for adherents and resin is considered for adhesive. Table 5 shows the material properties of adherents and adhesive. Table 6 shows the ratio  $K_\sigma/K_{\sigma|t/W=1}$  at the joint of interface when adhesive thickness  $t/W = 0.001, 0.01, 0.1, 0.5, 2, 4$ . Figure 11 is the figure for Table 6. It is found that  $F_\sigma/F_{\sigma|t/W=1}$  increases with increasing  $t/W$  until  $t/W = 1$ , and when  $t/W > 1$ ,  $F_\sigma/F_{\sigma|t/W=1}$  keeps constant 1.0, whatever the material combination is.

Generally, the Young's modulus  $E_2$  of adhesive is smaller than the Young's modulus  $E_1$  of adherent:  $E_2 \leq E_1$ , and the Poisson's ratio  $\nu_2$  of adhesive is larger than the Poisson's ratio  $\nu_1$  of adherent:  $\nu_2 \geq \nu_1$ . In this case, it is found that  $\alpha \geq 0$  and  $\alpha - 2\beta \geq 0$  and therefore singularity stress exists around the edge of interface. According to the values in Table 4, Fig.12 shows the variation of logarithmic  $F_\sigma/F_{\sigma|t/W=1}$  and  $t/W$  from  $\beta = -0.2$  to  $\beta = 0.4$  with different  $\alpha$ . It is found that  $F_\sigma/F_{\sigma|t/W=1}$  increases with increasing  $t/W$  until  $t/W = 1$  for all the material combinations when  $\alpha \geq 0$  and  $\alpha - 2\beta > 0$ . To improve the interface strength, thin adhesive layers are desirable because the intensity of singular stress decreases with decreasing the thickness.

Also, It should be noted that  $F_\sigma/F_{\sigma|t/W=1} = 1$  when  $\alpha - 2\beta = 0$  and  $F_\sigma/F_{\sigma|t/W=1}$  decreases with decreasing  $t/W$  when  $\alpha \geq 0$  and  $\alpha - 2\beta > 0$ .

Table 5 Material properties

	Material	Elastic Modulus/Gpa	Poissons ratio
Adherent	SUS304 (stainless steel )	206	0.3
	A7075 (aluminum alloys )	71	0.33
	Silicon	166	0.26
	FR-4.5 (IC substrate)	15.34	0.15
Adhesive	Resin	2.74	0.38

Table 6  $F_\sigma/F_{\sigma|t/W=1}$  with varying adhesive thickness  $t/W$

$t/W$	SUS304	A7075	Silicon	FR-4.5
0.001	0.100	0.118	0.102	0.229
0.01	0.212	0.236	0.215	0.355
0.1	0.466	0.4884	0.468	0.573
0.5	0.898	0.903	0.898	0.916
1	1.000	1.000	1.000	1.000
2	1.002	1.002	1.002	1.003
4	1.002	1.002	1.002	1.003

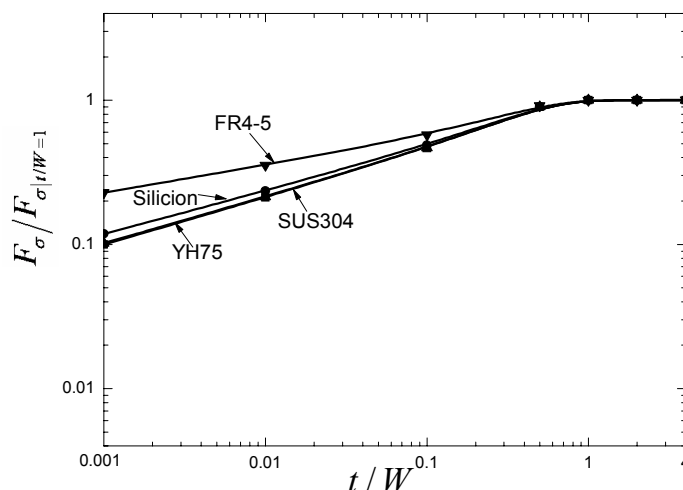


Fig.11  $F_\sigma/F_{\sigma|t/W=1}$  with varying adhesive thickness  $t/W$

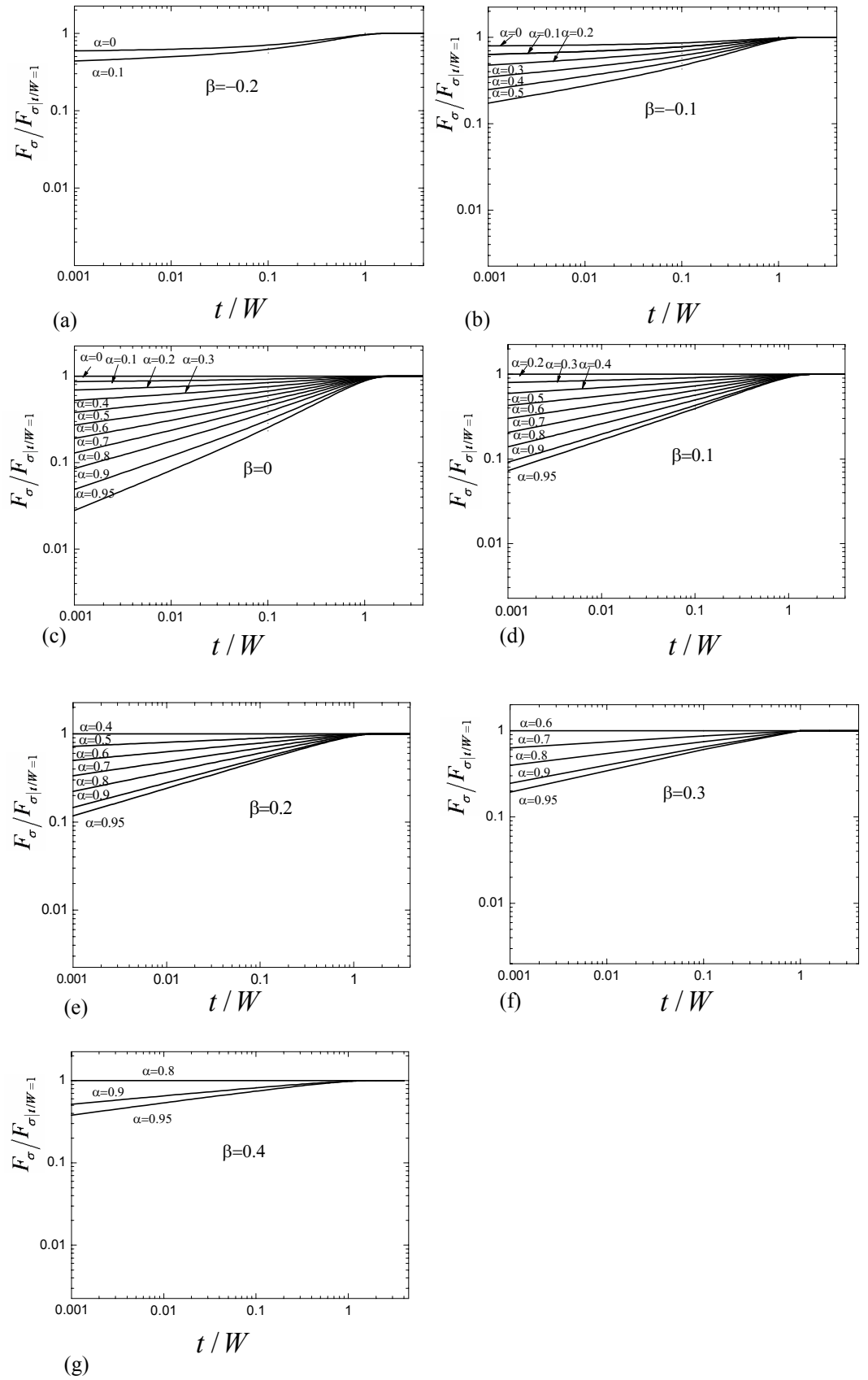


Fig.12  $F_{\sigma}/F_{\sigma|_{t/W=1}}$  with  $t/W$ . (a)  $\beta = -0.2$ ; (b)  $\beta = -0.1$ ; (c)  $\beta = 0$ ; (d)  $\beta = 0.1$ ; (e)  $\beta = 0.2$ ; (f)  $\beta = 0.3$ ; (g)  $\beta = 0.4$

## 6. Conclusions

In this paper the intensity of singular stress at the edge of adhesive dissimilar joint was discussed with varying the adhesive thickness and material combinations. The conclusions can be made in the following way.

(1) Accurate method for calculating the intensity of singular stress was proposed by using FEM. It is found that the ratio of intensity of singular stress  $K_{\sigma}^1/K_{\sigma}^2$  can be obtained from the ratio  $\lim_{r \rightarrow 0} (\sigma_{\theta}^1|_{\theta=\pi/2} / \sigma_{\theta}^2|_{\theta=\pi/2})$ . It is also found that the ratio  $K_{\sigma} / K_{\sigma|t/W=1}$  is constant along the interface if suitable FEM mesh is applied. Therefore, only the first node can be considered when the ratio of  $K_{\sigma} / K_{\sigma|t/W=1}$  is calculated.

(2) For a fixed value of  $\beta$ , it is found that  $K_{\sigma}$  increases with increasing  $\alpha$  when  $\alpha$  is small. On the other hand,  $K_{\sigma}$  decreases with increasing  $\alpha$  when  $\alpha$  is large. The range of intensity of singular stress  $K_{\sigma}$  is different depending on the adhesive thickness  $t/W$ .

(3) To improve the interface strength, thin adhesive layers are desirable because the intensity of singular stress  $K_{\sigma}$  decreases with decreasing the thickness. The increment is different depending on material combination. The ratio  $K_{\sigma} / K_{\sigma|t/W=1} = 1$  when  $t/W \geq 1$  whatever the material combination is.

## References

- (1) Kanno, T., Ogata, M., and Foxton, R.M., etc., Microtensile Bond Strength of Dual-cure Resin Cement to Root Canal Dentin with Different Curing Strategies, *Dental Material*, Vol.23, No.4 (2004), pp.550-556.
- (2) Kitasako, Y., Burrow, M.F., and Nikaido, T., etc., Shear and Tensile Bond Testing for Resin Cemented with Six Luting Agents, *The Journal of Prosthetic Dentistry*, Vol.80(1995), pp.423-428.
- (3) Van Meerbeek, B., De Munck, J., and Yoshida, Y., etc., Buonocore Memorial Lecture-Adhesion to Enamel and Dentin: Current Status and Future Challenges, *Operative Dentistry*, Vol.28(2003), 215-235.
- (4) Park, J.H., Choi, J.H., and Kweon, J.H., Evaluating the Strengths of Thick Aluminum-to-Aluminum Joint with Different Adhesive Lengths and Thicknesses, *Composite Structures*(2009), pp.1-10.
- (5) Arenas, J., Narbon, J.J., and Alia, C., Optimum Adhesive Thickness in Structural Adhesive Joints Using Statistical Techniques based on Weibull Distribution, *International Journal of Adhesion & Adhesives* (2009), pp.1-6.
- (6) Neves, A.A., Courinho, E., and Poitevin, A., Influence of Joint Component Mechanical Properties and Adhesive Layer Thickness on Stress Distribution in Micro-tensile Bond Strength Specimens, *Dental Materials*, Vol.25(2009), pp.4-12.
- (7) Afendi, M., and Teramoto, T., Fracture Toughness Test of Epoxy Adhesive Dissimilar Joint with Various Adhesive Thickness, *Proceedings of Asian Pacific Conference for Materials and Mechanics* (2009), a55.
- (8) Bogy, D.B., Edge-Bonded Dissimilar Orthogonal Elastic Wedges under Normal and Shear Loading, *Journal of Applied Mechanics*, Vol. 35, (1968), pp. 460-466.
- (9) Bogy, D.B., Two Edge-Bonded Elastic Wedges of Different and Wedge Angles under Surface Traction, *Journal of Applied Mechanics*, Vol. 38, (1971), pp. 377-386.
- (10) Chen, D.H., and Nisitani, H., Intensity of Singular Stress Field near the Interface Edge Point of a Bonded Strip, *Transactions of Japan Society of Mechanical Engineering*, A-59(567) (1993), pp.2682-2686.
- (11) Noda, N.A., Shirao, R., Li, J. and Sugimoto, J.S., Intensity of Singular Stress at the End of a Fiber under Pull-out Force, *International Journal of Solids and Structures*, Vol. 44, No.13(2007), pp.4472-4491.